

Positron studies of polycrystalline TiC

This article has been downloaded from IOPscience. Please scroll down to see the full text article.

1995 J. Phys.: Condens. Matter 7 9091

(<http://iopscience.iop.org/0953-8984/7/47/025>)

View [the table of contents for this issue](#), or go to the [journal homepage](#) for more

Download details:

IP Address: 171.66.16.151

The article was downloaded on 12/05/2010 at 22:33

Please note that [terms and conditions apply](#).

Positron studies of polycrystalline TiC

G Brauer†, W Anwand†, E-M Nicht†, P G Coleman‡, A P Knights‡, H Schut§, G Kögel|| and N Wagner¶

† Positron Group of TU Dresden at Research Centre Rossendorf Inc., PO Box 510119, D-01314 Dresden, Germany

‡ School of Physics, University of East Anglia, Norwich NR4 7TJ, UK

§ Interfaculty Reactor Institute, Delft University of Technology, Mekelweg 15, NL-2629 JB Delft, The Netherlands

|| Institut für Nukleare Festkörperphysik, Universität der Bundeswehr München, Werner-Heisenberg-Weg 39, D-85577 Neubiberg, Germany

¶ Fachbereich Physik, Martin-Luther-Universität Halle-Wittenberg, Friedmann-Bach-Platz 6, D-06108 Halle/Saale, Germany

Received 2 August 1995

Abstract. The mean positron lifetime τ , positron diffusion length L , and the positron and electron work functions (ϕ_+ and ϕ_-) for polycrystalline TiC have been experimentally determined. The results were $\tau = 160(2)$ ps, $L_+ = 138(27)$ nm and $\phi_- = 3.96(0.08)$ eV; ϕ_+ was shown to be almost certainly positive. These results strongly support the suggestion from recent first-principles electronic structure and positron state calculations that positions are trapped by and annihilate in metal vacancies in this material. XPS measurements indicate that the trapping sites may be predominantly in thin carbon-rich layers between grains, a picture which may also explain the long near-surface diffusion length.

1. Introduction

Refractory metal carbides and nitrides are attractive both for theoretical investigations and technological applications because of their interesting physical properties—e.g., high melting points, extreme hardness and relatively high superconducting transition temperatures [1–4]. Many of their desirable characteristics are critically influenced by the presence of vacancies, which occur mostly on the non-metal sublattice.

Positron annihilation spectroscopy (PAS) is a powerful tool for the investigation of defects with below-average electron density, particularly vacancies and vacancy clusters (voids), and can give also useful information about precipitates [5, 6]. From PAS studies of metals it is known that monovacancies are detected at concentrations as low as 0.1 ppm, dislocations from 10^{12} m⁻², and voids (with, say diameter 4.5 nm) from 2×10^{-8} per atom. Voids in metals can be detected and identified by positrons up to a size that corresponds to the agglomeration of about 50 monovacancies. Thus it is possible to study by PAS microstructural defects not detected by transmission electron microscopy. Whereas interstitial atoms and stacking faults are not directly seen by positrons, it is in some cases experimentally possible to distinguish free monovacancies from those bound to impurity atoms.

Due to the larger variety of defects in alloys and intermetallic compounds, the interpretation of PAS data is more difficult than for pure metals. Different types of defect may coexist and it is very hard to resolve their sometimes competing roles in the physical

processes studied. In most cases the only way to understand experimental PAS data in more complicated systems, and hence achieve a correct description of their defect characteristics, is to perform first-principles electronic structure and positron state calculations. Such calculations have recently been performed for several transition metal carbides and nitrides having either perfect NaCl structure or containing metal or carbon/nitrogen vacancies [7]. The quantities studied were the positron affinity A_+ and lifetime τ . The comparison of the calculated positron lifetimes with experimental data for group IV and group V refractory metal carbides [8] shows that even in highly stoichiometric systems positrons are annihilated mainly at vacancies. From the calculations it is also suggested that positrons are trapped and annihilated at metal vacancies, the existence of which is difficult to see by other experimental methods. The calculated positron affinities are important parameters in the interpretation of PAS results for materials containing carbide or nitride precipitates. A discussion about irradiation-induced precipitates in reactor pressure vessel steels, which might consist of carbides and/or nitrides, is published elsewhere [9–11].

The primary goal of the present work is the experimental verification of calculated positron properties of refractory metal carbides and nitrides applied to the case of polycrystalline TiC.

2. Experimental details

2.1. Sample preparation

The TiC sample was prepared by means of solid state vacuum reaction at high temperatures in the Institute of Solid State Chemistry of the Russian Academy of Sciences, Jekaterinburg. The original sample size was $8 \times 8 \times 1$ mm. This sample was broken into three pieces which were numbered as shown in figure 1.

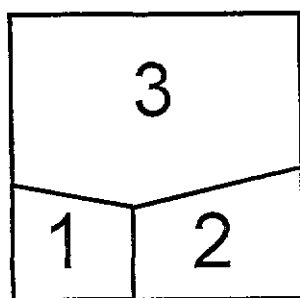


Figure 1. TiC sample showing pieces 1, 2 and 3; original dimensions 8×8 mm. Pieces 1 and 2 were used for lifetime and electron work function measurements, while piece 3 was used for positron beam measurements.

The lattice parameters of pieces 1 and 2, determined by x-ray diffraction, were 0.4316 and 0.4319 nm (both ± 0.0002 nm), respectively. The value registered at the International Centre for Diffraction Data (ICDD) [12] is 0.4327 nm; the fact that the measured lattice parameters are slightly smaller than the ICDD value (which is for a unit cell with the ideal stoichiometric composition) points to an inward relaxation of the crystal lattice due to the presence of vacancies. However, it is impossible to conclude from these data whether the

vacancies are metal and/or carbon. The correlation between the carbon content of TiC and the lattice parameter a is given in [13], which reports that TiC has a very wide homogeneity region ranging from 28 at% C ($a = 0.4269$ nm) to 50 at% C ($a = 0.4327$ nm); consequently the carbon content of the present TiC sample should be slightly smaller than for an ideal stoichiometric composition.

2.2. Measurements

For the positron lifetime measurements a 0.2 MBq $^{22}\text{NaCl}$ positron source was deposited on 2 μm Ti foils and sandwiched between TiC pieces 1 and 2. The lifetime measurements were performed by means of a γ - γ spectrometer equipped with BaF_2 scintillators and with a time resolution FWHM of 188 ps. The positron lifetime spectra with 9×10^6 coincidence counts were subjected to multicomponent fitting [14] and a variance of 1.06 was achieved. Because of the small specimen size about 27% of all annihilations occurred in the acrylic glass specimen holder. This source contribution (386 ps at 18.1% and 1736 ps at 8.2%) was determined precisely by measuring the annihilations in the empty sample holder under identical conditions. The appropriately corrected TiC decay spectrum exhibited only a single lifetime of 162 (2) ps. The intensity of any additional components cannot exceed 10% for lifetimes below 100 ps and 3% for lifetimes in excess of 300 ps.

Positron diffusion and re-emission from piece 3 were studied using the computer-controlled magnetically guided slow positron beam at UEA Norwich [15]. Positrons of controllable energies in the range 0.1–30 keV were guided to the target sample through a flight tube evacuated to 10^{-8} Torr; the beam diameter was reduced by an aperture of 4 mm diameter. The mean Doppler-broadened annihilation lineshape parameter S was measured as a function incident positron energy E .

Fitting of $S(E)$ data in terms of depth-dependent material parameter is an even more complicated task than the fitting of positron lifetime spectra referred to above. In positron beam profiling measurements it is generally difficult to indicate what contribution the positrons implanted at certain depth make to the measured lineshape parameter S because combined diffusion and trapping processes might be involved. Moreover, at low incident energies epithermal positrons might be present which behave differently from thermalized positrons.

The extraction of reliable depth-sensitive information depends on the use of the correct form of the implantation profile $P(z, E)$ to describe the initial distribution of depths z below the surface of positrons incident with energy E . Implantation depth here is defined as the depth reached after thermalization and prior to any subsequent diffusion. This implantation profile can be parametrized fairly well, for uniform materials without high defect concentration, by a Makhov distribution as follows:

$$P(z, E) = (m/z_0)(z/z_0)^{m-1} \exp[-(z/z_0)^m] \quad (1)$$

where $z_0 = (A/\rho)E^n$, with E in keV, ρ the density of the material in g cm^{-3} , and A , m , and n material-independent parameters. Vehanen *et al* [16] obtained experimental values for the latter parameters of $A = 4.5(0.3) \mu\text{g cm}^{-2} \text{keV}^{-1.62}$, $m = 2(0.1)$, and $n = 1.62(0.05)$.

The time-averaged positron density $c(z)$ at a certain depth z below the solid surface can be found from the balance between positron stopping, positron diffusion, bulk annihilation and trapping at defects from the diffusion equation

$$D_+ \frac{d^2c}{dz^2} - \frac{d(v_d c)}{dz} + I(z) - \kappa_i n_i c - \lambda_b c = 0 \quad (2)$$

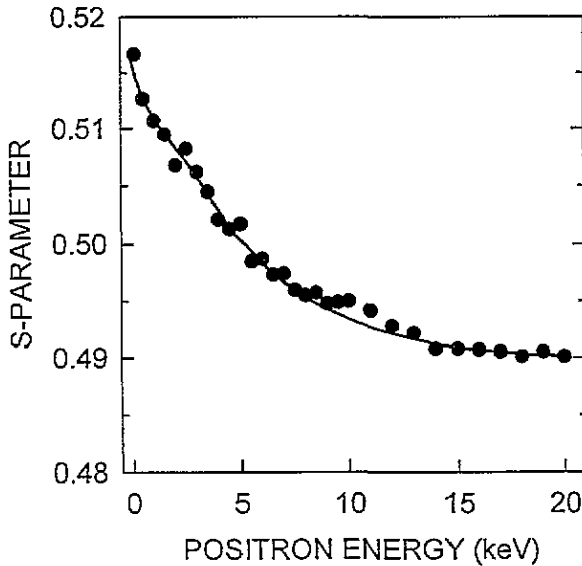


Figure 2. The mean S -parameter versus incident positron energy for TiC piece 3. The solid circles represent experimental data; the solid line represents the fit obtained using VEPFIT (see the text).

where $v_d(z) = \mu E(z)$ = drift velocity (μ = positron mobility, E the electric field strength); $I(z)$ = positron stopping rate at depth z (density increase s^{-1}); $n_t(z)$ = defect density; κ_t = rate constant for positron trapping at defects; and D_+ = positron diffusion constant.

Several methods have been suggested in the literature to separate the effects due to epithermal positrons from those due to thermalized positrons [17, 18]; one of these methods is applied in the program VEPFIT [19] which is applied here to the extraction of relevant parameters from the slow positron measurements on TiC.

The most common experimental methods for estimating the electron work function of metal surfaces are either contact potential (CP) measurements (Kelvin probe or electron tube in residual current region mode) or thermionic, photo- and field emission methods [20]. Here, in a two-electrode tube under HV conditions, a tungsten tip was positioned as reference electrode in front of the TiC surface being studied, which was cleaned in HV ($< 10^{-5}$ Pa) and annealed at 500 °C to reduce any possible adsorbate dipole contribution to the work function. Measurements of the contact potential U_{CP} via stable tube current (indicating a clean and well-defined surface) were performed as a function of applied voltage (see figure 3). The difference in work functions of the tungsten probe (ϕ_w) and the sample surface (ϕ_-), with e being the elementary charge of the electron, is thus

$$U_{CP} = (\phi_- - \phi_w)/e. \quad (3)$$

Applying the Richardson formula [18] to experimental data ϕ_w was deduced and thus ϕ_- was found from equation (3).

The positron work function, if negative, is determined by measuring the maximum energy of slow positrons re-emitted from a surface. For TiC this was attempted by employing simple retarding-potential energy analysis; the largest TiC piece (3) was mounted on top of a copper backplate and sputtered and annealed in UHV. A piece of annealed tungsten foil was suspended below the samples. The smallest diameter beam available (4 mm) was used and the annihilation count rate measured as a function of sample bias.

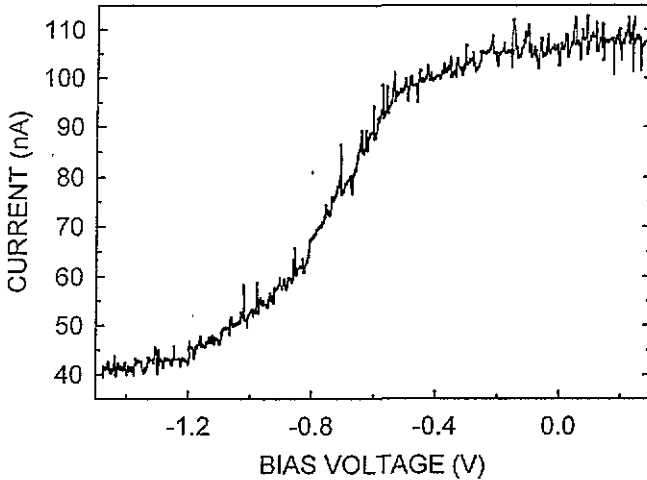


Figure 3. The residual/saturation current versus bias voltage used to determine the electron work function for TiC piece 2.

3. Results and discussion

The data for TiC that might be verified experimentally, based on the first-principles electronic structure and positron state calculations for perfect and imperfect transition metal carbides and nitrides [7], are collected in table 1. Measurement of the positron lifetime τ is direct; the positron affinity A_+ is connected to the positron work function ϕ_+ and electron work function ϕ_- by [21]:

$$A_+ + \phi_+ + \phi_- = 0. \quad (4)$$

Table 1. Calculated positron affinities A_+ and lifetimes τ of TiC [7]. TiC denotes the perfect lattice, whereas Ti_3C_4 and Ti_4C_3 denote the lattices with metal and carbon vacancies, respectively.

Material	A_+ (eV)	τ (ps)
TiC	-1.8	98
Ti_3C_4	-7.6	161
Ti_4C_3	-3.2	124

3.1. Positron lifetime

A mean positron lifetime of 160 ps for TiC was reported by Rempel *et al* [8], who assigned this value to the annihilation of positrons with metal valence electrons. However, in an extended discussion Puska *et al* [7] showed that a more likely interpretation of this result is based on positron trapping at and annihilation in metal vacancies. The earlier experimental data could not be decomposed reliably into several components, and so the measurement was repeated with improved time resolution and statistics.

We conclude from the new measurement that only one positron lifetime component of 162(2) ps is present in the TiC. By reference to table 1 it is evident that this result strongly supports our earlier conclusion [7] that positrons are annihilated at Ti vacancies in the TiC.

3.2. Positron diffusion length

The results of the $S(E)$ measurement for TiC (piece 3) are shown in figure 2, along with the results of fitting by the program VEPFIT referred to earlier. There is a small perturbation at low energies (\sim keV) associated with epithermal positrons, which is allowed for by VEPFIT. S decreases from its surface value of 0.511 (0.002) to the bulk value of 0.4895 (0.0015) before E reaches 20 keV, which leads to the fitted diffusion length L_+ of 138 (27) nm. The positron diffusion constant D_+ is related to L_+ by

$$D_+ = (\lambda + n\nu)L_+^2 \quad (5)$$

where λ is the bulk annihilation rate, n is the defect number density and ν the specific trapping rate. Therefore the ratio of diffusion lengths in perfect and defected samples is given by

$$(L_+)_{\text{perfect}} / (L_+)_{\text{defected}} = [(\lambda + n\nu)/\lambda]^{1/2}. \quad (6)$$

Now it can be straightforwardly shown from the two-state trapping model that the fraction of positrons trapped by defects, f , is $n\nu/(\lambda + n\nu)$; thus the right-hand side of equation (6) reduces to $[1 - f]^{1/2}$. We can estimate that the value of f must be at least 0.9–0.95 so that only one lifetime—that attributed to positrons annihilated in Ti vacancies—is seen in the lifetime experiment referred to above, so the ratio of diffusion lengths in equation (6) is about 4. This implies that L_+ in ‘perfect’ TiC would be 400–500 nm, a very large value—2–4 times the typical values for metals and 1.5–2 times those reported for semiconductors. (D_+ would be 15–25 cm² s⁻¹—again much larger than values quoted for other materials.) To investigate this apparent anomaly the stoichiometry of sample 3 was studied by the application of x-ray photoemission spectroscopy, as described in section 3.4 below.

3.3. Positron and electron work functions

No evidence of work function positron emission from TiC was observed; a small step in the integral count rate data close to zero sample bias was attributed on close examination to positron re-emission from the copper backplate, which was unavoidably hit by some of the incident positrons. There was, however, some evidence of epithermal emission. The conclusion from this work is that the positron work function is almost certainly positive.

Using the Richardson formula, as outlined in section 2 above, a value of 4.5 eV was found for the electron work function of tungsten. As a check, the same method was used to determine a value for the electron work function for graphite of 4.55 eV—in good agreement with the literature [22, 23]. The results of the electron work function measurements for the three pieces of TiC were: 3.88, 3.98 and 4.03 eV.

The calculated affinities (table 1) and measured electron work functions result in a positive positron work function (via equation (4)) only in the case of metal vacancies in the TiC material. Alternatively, one could say that positrons bound to vacancies cannot be re-emitted into the vacuum because their binding energy (table 1) is too large for thermally induced detrapping at ambient temperature. Whereas the present study indicates only that the positron work function is indeed positive, experimental determination of its value could be performed by positronium time-of-flight measurements. Because this is technically difficult a new method has been proposed [24] in which ϕ_- is deduced from the positron-induced secondary electron spectrum. Measurements are being pursued at the electrostatic slow positron beam commissioned recently at the University of Texas at Arlington.

3.4. X-ray photoemission spectroscopy (XPS) results

The carbon content of the present TiC sample should be slightly smaller than that for ideal stoichiometric composition (see 2.1); however, in the case of polycrystalline structures this statement needs to be put into perspective. If the crystallites are connected by defect-rich boundaries which represent inner interfaces then the adjustment to thermodynamically favoured equilibrium states might be hindered. Such a structure is suggested by the electron micrograph of sample 3 shown in figure 4. The line scan of the Ti secondary-electron distribution suggests a rather even distribution on the scale of grain sizes. However, to describe the distribution of Ti in the crystallite itself in more detail further microanalytic investigations are necessary.

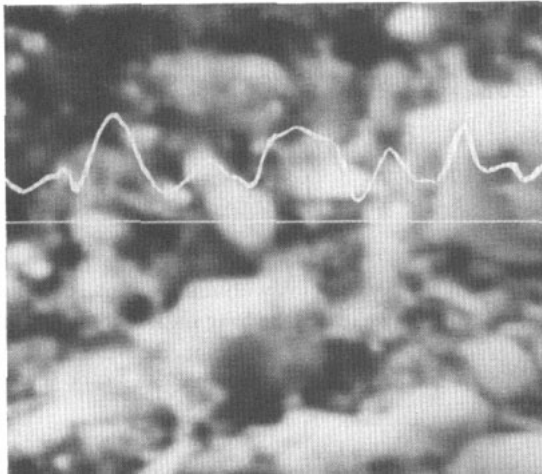


Figure 4. A scanning electron micrograph of sample 3, showing the topography of the surface. The magnification is 10000:1. The width of the image is 10 μm . The white line is a line-scan of the Ti distribution.

The premise that polycrystalline TiC has a structure whose inhomogeneity is due to the presence of structural defects was illustrated by the results of a simple XPS experiment performed on sample 3. For the untreated sample only one photoemission peak, corresponding to an electron binding energy $E_B = 285.0$ eV, was observed in the energy range characteristic of C_{1s} core levels. This value of E_B is in contrast with the value of 281.7 eV expected for carbon in TiC. Taking into account the escape depth of the photoelectrons the existence of a carbon-rich deposit—containing structures such as Ti_3C_4 —of at least 10 nm depth can be postulated.

This conjecture was further studied by sputtering the sample with 500 eV Ar^+ ions ($1 \mu\text{A cm}^{-2}$ at 10^{-7} mbar for 30 min). The appearance of a peak at 281.7 eV, as shown in figure 5(a), indicates that some TiC had been revealed. The sample was then heated to 400 K in UHV and the spectrum shown in figure 5(b) was obtained. The substantial enhancement of the peak at 285.0 eV is attributed to the diffusion of segregated carbon from carbon-rich inner interfaces to replace that lost by sputtering.

It may be concluded that the process of producing polycrystalline TiC, which is controlled by reaction kinetics, leads to a Ti deficiency at grain surfaces—seen by positrons

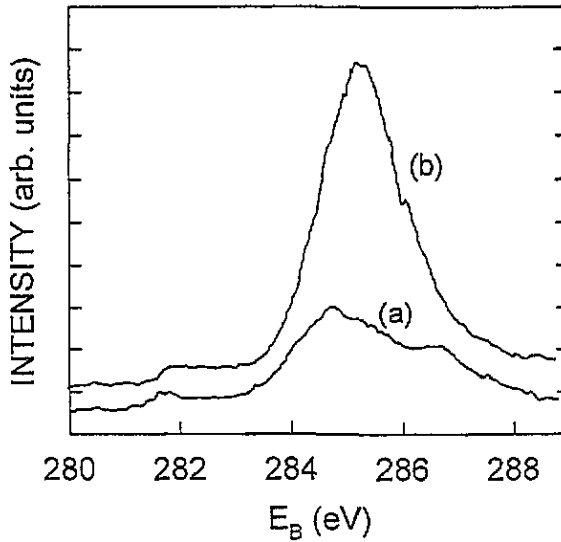


Figure 5. XPS spectra for sample 3: (a) after Ar-ion sputtering; and (b) after heating the sputtered sample to 400 K. The peaks at 281.7 eV corresponds to C in TiC.

as Ti vacancies—and the corresponding C vacancies within the grains. Unhindered diffusion of positrons through subsurface grains may explain the long measured diffusion length; in the bulk, positrons diffuse across grains but are efficiently trapped in the carbon-rich interface regions at their boundaries.

4. Conclusions

The present results demonstrate the usefulness of positron spectroscopies, in conjunction with established complementary techniques, in the extraction and verification of the properties of materials such as TiC. Taken together, the experimental results strongly support the proposition [7] that in TiC positrons are preferentially trapped by metal vacancies, whose existence in this class of materials has been in some doubt [25]. Direct evaluation of the positron work function by further experiments can help to support this conclusion. XPS results, together with a long measured diffusion length, suggest that the positron sees Ti vacancies in thin C-rich layers at the grain boundaries. In order to probe bulk TiC the use of single-crystal specimens will therefore be required in future experiments. Another possibility could be the use of a positron microbeam with $\sim \mu\text{m}$ diameter; encouraging progress in this direction has been reported recently [26,27].

Acknowledgment

The TiC sample was kindly supplied by A A Rempel and A I Gusev from the Institute of Solid State Chemistry of the Russian Academy of Sciences at Jekaterinburg.

References

- [1] Toth L E 1971 *Transition Metal Carbides and Nitrides* (New York: Academic)
- [2] Schwarz K 1987 *Crit. Rev. Solid Mater. Sci.* **13** 211
- [3] Gusev A I 1991 *Phys. Status Solidi b* **163** 17
Gusev A I and Rempel A A 1993 *Phys. Status Solidi a* **135** 15
- [4] Rempel A A 1992 *Ordering Effects in Non-stoichiometric Interstitial Compounds* (Ekaterinburg: Nauka, Ural Division) (in Russian)
- [5] Hautojärvi P (ed) 1979 *Positrons in Solids (Springer Topics in Current Physics 12)* (Berlin: Springer)
- [6] Brandt W and Dupasquier A (ed) 1983 *Positron Solid-State Physics, Proc. Int. School of Physics 'Enrico Fermi', Course LXXXIII (Varenna, 1981)* (Amsterdam: North-Holland)
- [7] Puska M J, Sob M, Brauer G and Korhonen T O 1994 *Phys. Rev. B* **49** 10947
- [8] Rempel A A, Forster M and Schaefer H-E 1993 *J. Phys.: Condens. Matter* **5** 261
For a more detailed presentation see
Rempel A A, Forster M and Schaefer H-E 1992 *Dokl. Adam. Nauk SSR* **326** 91
- [9] Brauer G, Sob M and Puska M J 1992 *Mater. Sci. Forum* **105-10** 611
See also [10].
- [10] Brauer G, Puska M J, Sob M and Korhonen T O 1995 *Nucl. Eng. Design* **158** 151
The values of positron affinities and lifetimes in this reference differ slightly from those given in the preliminary report [9] due to a better self-consistency and more accurate positron potential
- [11] Brauer G 1995 *J. Physique IV, Coll. C1* 143 (supplement to *J. Physique III* 5)
- [12] International Centre for Diffraction Data, 1601 Park Lane, Swarthmore, PA 19081, USA.
- [13] Pearson W B 1964 *A Handbook of Lattice Spacings and Structures of Metals and Alloys (Int. Series of Monographs on Metal Physics and Physical Metallurgy 4)* ed G V Raynor (Oxford: Pergamon) pp 949, 960
- [14] Kirkegaard P and Eldrup M 1974 *Comput. Phys. Commun.* **7** 401
- [15] Chilton N B and Coleman P G 1995 *Meas. Sci. Technol.* **6** 53
- [16] Vehanen A, Saarinen K, Hautojärvi P and Huorno H 1987 *Phys. Rev. B* **35** 4606
- [17] Huorno H, Vehanen A, Bentzon M B and Hautojärvi P 1987 *Phys. Rev. B* **32** 8252
- [18] Britton D T, Rice-Evans P C and Evans J H 1988 *Phil. Mag. Lett.* **57** 165
- [19] van Veen A, Schut H, de Vries J, Hakvoort R A and Ijzma M R 1990 *Positron Beams for Solids and Surfaces* ed P J Schultz, G R Massoumi and P J Simpson (New York: American Institute of Physics) p 171
- [20] Hölzl J and Schulte F K 1979 *Solid Surface Physics (Springer Tracts in Modern Physics 85)* (Berlin: Springer) and references therein
- [21] Puska M J, Lanki P and Nieminen R M 1989 *J. Phys.: Condens. Matter* **1** 6081
- [22] Michelson H B 1977 *J. Appl. Phys.* **48** 4729
- [23] Johansson L I, Hagström A L, Jacobsen B E and Hagström S B M 1977 *J. Electron Spectrosc. Relat. Phenom.* **10** 267
- [24] Weiss A H, Yang S, Zhou H Q, Jung E, Koymen A R, Naidu S, Brauer G and Puska M J 1995 *Appl. Surf. Sci.* **85** 82
- [25] See, for example,
Gubanov V A, Ivanosky A L, Shveikin G P and Ellis D E 1984 *J. Phys. Chem. Solid* **45** 719
Marksteiner P, Weinberger P, Neckel A, Zeller R and Dederichs P H 1986 *Phys. Rev. B* **33** 812
- [26] Zecca A, Brusa R S, Duarteñaia M P, Karwasz G P, Paridaens J, Piazza A, Kögel G, Sperr P, Britton D T, Uhlmann K, Willutzki P and Triftshäuser W 1995 *Europhys. Lett.* **29** 617
- [27] Goodyear A and Coleman P G 1995 *Appl. Surf. Sci.* **85** 98